Available on CMS information server **CMS AN -2008/114**

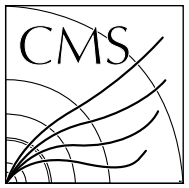

The Compact Muon Solenoid Experiment

Analysis Note

The content of this note is intended for CMS internal use and distribution only

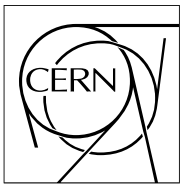

22 December 2008

Extending the early SUSY search with all-hadronic dijet events to n-jet topologies.

T. Whyntie, O. Buchmüller, H. Flächer, J. Jones, T. Rommerskirchen, M. Stoye, A. Tapper

Abstract

We present a status update on the analysis efforts aimed at extending the all-hadronic dijet SUSY search with the CMS detector at the LHC to event topologies containing n hadronic jets. We have reinterpreted the α_T observable, as defined in the dijet analysis, and applied it to a *pseudo-dijet* formed by merging the n jets in such a way that the difference between the transverse energy of the resulting pseudo-jets is minimised. The initial results from a preliminary analysis using this method suggest that similar signal to background ratios as for the dijet analysis are possible, with each additional n jet system considered adding to the signal yield. The self-protection of α_T against mismeasurement of QCD events, as compared to a calometric E_T multijet search approach, is briefly investigated, and new α_T-like observables, based on similar kinematic variables, are discussed and briefly explored.

1 Introduction

The first non-Standard Model (SM) physics discoveries at the Large Hadron Collider (LHC) will face, at the very least, two challenges that must be addressed simultaneously. Firstly, the behaviour of SM background processes in the new energy regime will take time to understand and characterise. Early search strategies must therefore rely on assumptions based on simple physical principles or data-driven background estimation methods to confirm the presence of new physics. Secondly, factors such as detector noise and miscalibration will affect the quality of early data. For example, calometric $\not\!\!E_T$ measurements rely on having a complete understanding of the calorimetry system, which will also take time. Searches carried out in the initial phases of machine operation should therefore aim to be robust against these uncertainties.

An example of such a strategy for the all-hadronic SUSY search channel is described in [1], building on work carried out in [2]. In certain regions of SUSY parameter space, pair-produced squarks each decay into a quark and a $\tilde{\chi}_1^0$, the Lightest Supersymmetric Particle (LSP). The resulting event topology consists of two high-p_T jets and a missing energy signature due to the two invisible neutralinos. Despite the overwhelming QCD dijet background, this channel looks promising thanks to the exploitation of kinematic properties of the dijet system. Other important backgrounds, such as $Z(\rightarrow \nu\bar{\nu}) +$ jets, where dijets are produced with a real missing energy, are constrained using the data driven methods described in [1]. After recalling some of the standard transverse-plane observables in Section 2, we discuss in Section 3 the kinematic discriminants used in the dijet analysis and recount some of the key features of the Monte Carlo-based analysis presented therein.

A natural extension of this search channel considers events containing n hadronic jets. This note aims to provide an update on the status of some of the analysis effort in this area. In Section 4 we suggest a search strategy for this channel where the n-jets are reduced to a *pseudo-dijet* system, to which an α_T-like variable is applied. Section 5 presents the results of a preliminary, unoptimised analysis performed on the Monte Carlo signal and background datasets featured in [1]. We have also embarked on an initial study of the properties of observables similar to α_T that may be useful in the context of early searches for new physics. In particular, we investigate whether α_T offers a degree of self-protection against jet mismeasurement in Section 5.1, and the generalisation of the α_T approach with the formulation of new observables based on similar kinematic variables in Section 6. The estimation of SM backgrounds due to real $\not\!\!E_T$ in the n-jet system is not discussed here and will be the subject of a future note. Finally, in Section 7 we present our conclusions and outline plans for future work.

2 Kinematics in the transverse plane

As is standard practice in hadron-hadron collider physics, we work in terms of the kinematic properties of objects in the x-y or *transverse* plane. As such, we define the following variables for our system of n (hadronic) jets j:

$$H_T = \sum_{i=1}^{n} E_T^{j_i} \tag{1}$$

sets the scale of the interaction in the transverse plane. Generally speaking, for final state objects it is assumed that $E_T^{j_i} = p_T^{j_i}$.

$$\not\!\!\mathbf{H}_T = -\sum_{i=1}^{n} \mathbf{p}_T^{j_i} = -\mathbf{h}_T, \tag{2}$$

where $\mathbf{p}_T^{j_i}$ is the vectorial projection of the object momentum in the transverse plane, describes the scale and direction of the missing transverse energy as defined by the n object system. We use a lower-case $\mathbf{h}$ to highlight the vectorial nature of $\not\!\!\mathbf{H}_T$ and $\mathbf{h}_T$. We contrast $\not\!\!\mathbf{H}_T$ with $\not\!\!E_T$, which considers the sum of all calometric measurements made in the detector.

$$M_{T(\text{Tot.})} = \sqrt{\left(\sum_{i=1}^{n} E_T^{j_i}\right)^2 - \left(\sum_{i=1}^{n} p_x^{j_i}\right)^2 - \left(\sum_{i=1}^{n} p_y^{j_i}\right)^2} = \sqrt{H_T^2 - |\not\!\!\mathbf{H}_T|^2} \tag{3}$$

represents the *transverse mass* of the system. We note that in a system where energy and momentum are conserved and all constituent objects are included and have been measured perfectly, which we define for the sake of argument as a *perfect* system, $|\not\!\!\mathbf{H}_T| = \not\!\!E_T = 0$, and M_T is at its maximal value, H_T.

Additionally, we define fake $\not\!\!\mathbf{H}_T$ as the $\not\!\!\mathbf{H}_T$ caused by mismeasurements in the detector or the exclusion of otherwise detectable objects by event preselection cuts. Real $\not\!\!\mathbf{H}_T$ is caused by losses due to objects that are, for all intents and purposes, undetectable by the experiment, e.g. neutrinos, LSPs, etc.

3 The dijet system - a special case

We now consider the hadronic dijet system of [1] and [2]. The observable used to reject most of the (simulated) QCD background after event preselection cuts, known as α_T, is defined as

$$\alpha_T = \frac{\text{min.}\left(E_T^{j_1},\, E_T^{j_2}\right)}{M_T^{j_1,\, j_2}}. \tag{4}$$

We can express this in terms of the variables defined in Section 2 by replacing the numerator with the following, equivalent, expression:

$$\alpha_T = \frac{\frac{1}{2}\left(E_T^{j_1} + E_T^{j_2} - \left|E_T^{j_1} - E_T^{j_2}\right|\right)}{M_T^{j_1,\, j_2}} \tag{5}$$

$$= \frac{\frac{1}{2}\left(H_T - \Delta H_T\right)}{\sqrt{H_T^2 - |\not{H}_T|^2}} \tag{6}$$

where $\Delta H_T = |E_T^{j_1} - E_T^{j_2}|$ is the difference between the transverse energies of the jets (which need not necessarily be ordered in E_T). Thus for a perfect dijet system (e.g. a QCD dijet event recorded with a fully-understood detector), $\Delta H_T = 0, \not{H}_T = 0$ and so $\alpha_T = 1/2$. In [1] a cut is therefore applied that rejects events with $\alpha_T < 0.55$ to allow for the finite resolution of jet measurements. Conversely, signal-like events with a real, large missing transverse energy comparable to the H_T of the event will produce small $M_{T(\text{Tot.})}$ values, and so will tend to pass the cut regardless of the difference between the jet transverse energies.

The plot of α_T for the low mass SUSY point LM1 [3] and the dominant backgrounds – QCD, $Z(\rightarrow \nu\bar{\nu}) +$ jets, ($t\bar{t}$, Z, W) + jets, etc. – for 1 fb^{-1} after the $H_T > 500$ GeV preselection cut is shown in Figure 1. Note the strong peak and sharp edge at $\alpha_T = 1/2$ for the QCD sample, and the large α_T values for the signal (and, to a lesser extent, the backgrounds with real $\not{H}_T$).

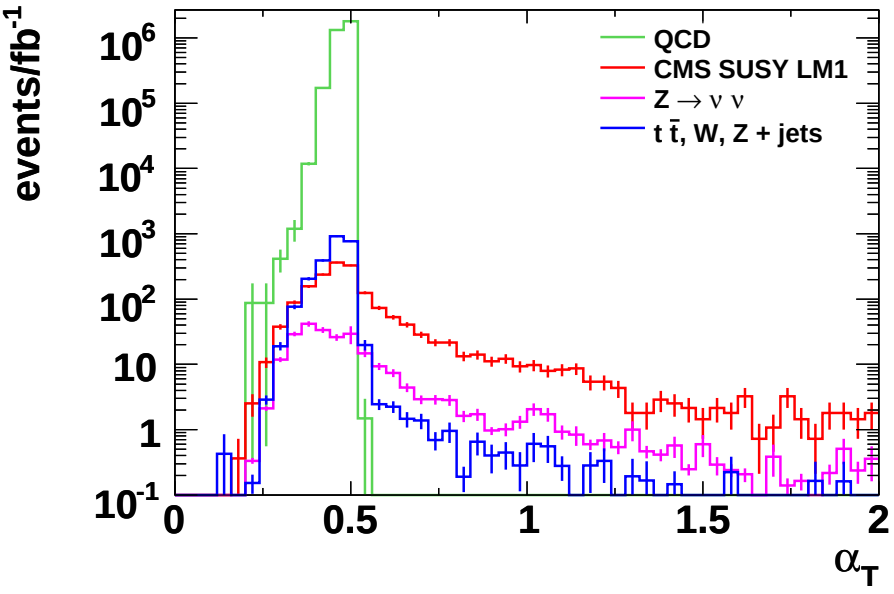

Figure 1: Plot of α_T for the hadronic dijet system after the preselection cuts up to and including $H_T > 500$ GeV, as outlined in [1].

Another kinematic variable explored in [1] is $\Delta\phi(j_1,\, j_2) = \Delta\phi\left(\mathbf{p}_T^{j_1},\, \mathbf{p}_T^{j_2}\right)$, the azimuthal angle between the two jets. This is a measure of the *acoplanarity* of the system. A further cut is applied after the α_T cut such that only events satisfying

$$\Delta\phi(j_1,\, j_2) < \frac{2\pi}{3}\,\text{rad}. \tag{7}$$

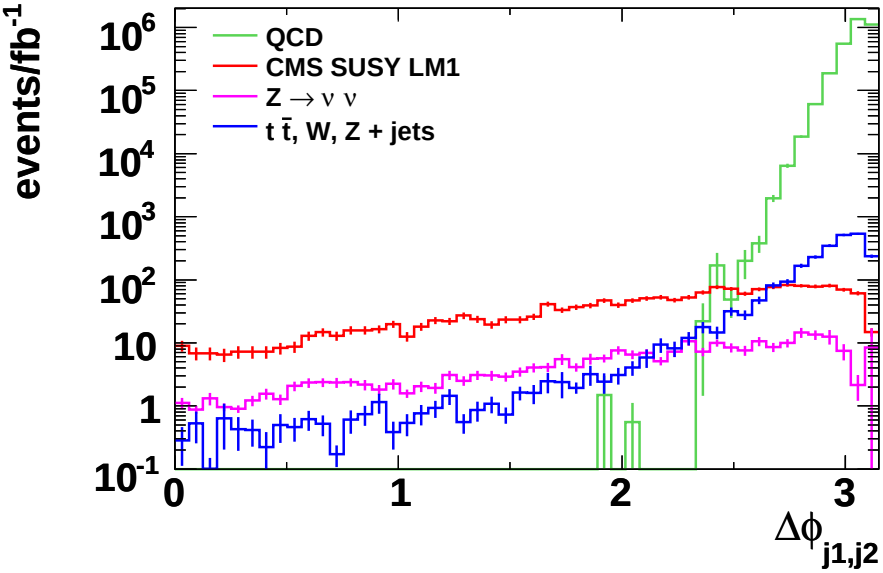

Figure 2: Plot of $\Delta\phi(j_1,\, j_2)$ for the hadronic dijet system after the preselection cuts up to and including $H_T > 500\,\text{GeV}$, as outlined in [1].

are accepted, with the aim of rejecting events with a back-to-back configuration. Figure 2 shows the plot of $\Delta\phi_{\,(1,\,2)}$ (again, for events passing the $H_T > 500\,\text{GeV}$ preselection cut, but without the $\alpha_T > 0.55$ requirement).

In [1] this cut is applied after the α_T cut, and as can be seen from Table 1, it makes very little difference to the final signal and background yields. This, along with the plot in Figure 2, suggests that the two variables contain very similar information in the dijet case; indeed, this relationship is explored in Section 5.1 of [1]. As we shall see in the following discussion of n-jet topologies, this makes the dijet system a somewhat special case.

Another cut used in the dijet analysis compares the direction of $\not{H}_T$ with those of the two selected jets ($E_T^{j_{1,2}} > 50\,\text{GeV}$) and a possible third jet with $30\,\text{GeV} < E_T^{j_3} < 50\,\text{GeV}$. An event is rejected if

$$\Delta\phi\,(\not{H}_T,\, \mathbf{p}_T^{j_i}) < 0.3\,\text{rad}. \tag{8}$$

where $i = 1, 2, 3$. This was employed as a check to make sure that any calculated $\not{H}_T$ was not simply a result of a severe mismeasurement of one of the main jets or the exclusion of a jet that sat just outside of the dijet cut definition ($E_T^j > 50\,\text{GeV}$, $F_{\text{EM}}^j < 0.9$). This is an interesting example of using a cut to protect against accepting events because of a mismeasurement or a self-imposed real missing E_T (due to, for example, exluding jets with the pre-selection cuts). We explore this concept further in Section 5.1.

The results for the dijet case are repeated for convenience in the $n = 2$ section of Table 1. The signal-to-background ratio after the $\alpha_T > 0.55$ and $0 < \Delta\phi(j_1,\, j_2) < 2\pi/3$ cuts is 5.6.

4 Extending the search to an n-jet system

The analysis of the hadronic dijet system reported in [1], combining the application of α_T and $\Delta\phi(j_1,\, j_2)$ with data-driven background estimation techniques, indicates that this search channel could be promising for early SUSY searches with the CMS experiment. A natural extension to the dijet channel arises from considering SUSY processes where the final state contains two LSPs and n hadronic jets, for example

$$pp \to \tilde{g}\tilde{q} \to \tilde{q}q\tilde{\chi}_1^0 q \to \tilde{\chi}_1^0 qq\tilde{\chi}_1^0 q, \tag{9}$$

where in this case $n = 3$. This increases the potential signal yield, which would be useful for searches using early data where machine energy and luminosity will be below the nominal design values. In order to do this, it is constructive to establish methods similar to those used in the dijet analysis for rejecting and/or estimating background processes. A suggested strategy is discussed below.

4.1 Extending the preslection cuts for n hadronic jets

In order to select events with a suitable n-jet topology, the following changes were made to the event preselection cuts described in [1]:

- An event is classified as an n jet system if it contains *exactly* n jets with $E_T^j > 50\,\text{GeV}$ and $F_{\text{EM}}^j < 0.9$;
- Any event containing a jet with $E_T^j > 50\,\text{GeV}$ and $F_{\text{EM}}^j > 0.9$ is rejected;
- The $\Delta\phi\,(\not{\mathbf{H}}_T,\, \mathbf{p}_T^j)$ cut (Equation 8) is applied to every jet up to and including the $(n+1)^{\,\text{th}}$ jet.

This defines our n-jet hadronic jet system. Note that the same requirements are placed on all n jets, with the exception of the cut on the η of the leading jet, $|\eta^{j_1}| < 2.5$.

4.2 The n-jet philosophy

With the n hadronic jets selected, the next step is to define a suitable discriminating variable upon which events are accepted or rejected. We have followed the approach of the dijet analysis by combining the n jets into a *pseudo-dijet* system and then applying the α_T and $\Delta\phi$ cuts to the pseudo-dijet. This is not an unreasonable approach to take, as the final state n jets will, generally speaking, be the result of some sort of cascade/showering from the initial two-body interaction. However, we should emphasise that this approach is an extension of the dijet analysis and should be regarded as such. When moving from n jets to two pseudo-jets, one must first choose how the n jets should be grouped into two jet collections, one for each pseudo-jet. One must then decide what metric to use to form the pseudo-jets out of each jet collection. For example, when $n = 3$, one could choose to always group the two softest jets into one pseudo-jet, and use 4-vector addition to merge these two jets together. A strategy we have found to work well is described in the next section.

4.3 Defining α_T for n jets

Firstly, we consider the denominator of α_T. Requiring that $M_T^{\text{Tot.}}$ should be same for the n jets considered individually or for any chosen pseudo-dijet system constructed from the n jets, we employ the following pseudo-jet merging scheme:

$$E_T^{jk} = E_T^j + E_T^k \tag{10}$$

$$p_x^{jk} = p_x^j + p_x^k \tag{11}$$

$$p_y^{jk} = p_y^j + p_y^k \tag{12}$$

Figuratively speaking, this is the equivalent of adding together the length of the $\mathbf{p}_T$ vectors (which, for massless objects, will have the same magnitude as the E_T) and pointing the resulting jet in the direction of the vectorial sum of the $\mathbf{p}_T$ vectors. Note that we must now consider the combined objects purely in the transverse plane.

Likewise, the numerator of α_T suggests a strategy for choosing the most appropriate jet combination. We notice that the ideal QCD dijet case, where $\alpha_T = 1/2$, is obtained when $\Delta H_T = 0$ and the jets are balanced in E_T. We therefore consider *all* possible combinations of $n \to 2$ jets and select the one that minimises ΔH_T. Figure 3 shows how, for example, this transverse energy clustering mechanism picks out the most dijet-like combination for the perfectly measured three jet case where the possible combinations are $\{1,\,23\}$, $\{2,\,13\}$ and $\{3,\,12\}$. Note that while for three jet systems, $\{1,\,23\}$ (where the jets are ordered by E_T) will always pick out the smallest ΔH_T, there is no such rule for $n \geq 4$. For example, there is no way to tell without explicit calculation whether $\{14,\,23\}$ or $\{1,\,234\}$ will yield the smaller ΔH_T value. This is why all combinations must be considered in the general n-jet case. We also note that ΔH_T will increase as the angles between the component jets of the pseudo-jet increase, and that ΔH_T is not necessarily zero for an $n > 2$ jet system, as even small opening angles between jets that are merged will produce a larger (and so imbalanced) E_T^{jk}. Thus the definition we arrive at for the n-jet α_T is

$$\alpha_T = \frac{\frac{1}{2}\left(H_T - \Delta H_{T(n)}\right)}{\sqrt{H_T^2 - |\not{\mathbf{H}}_T|^2}}\,, \tag{13}$$

where $\Delta H_{T(n)}$ is the minimum ΔH_T obtained by considering all possible $n \to 2$ jet combinations. Another way to think about $\Delta H_{T(n)}$ is as follows: if we were to try and place the transverse energies of the n hadronic jets

onto the two pans of a weighing scale, each pan representing a pseudo-jet, ΔH_T would be difference in E_T of the most balanced combination. It is important here to emphasise the fact that this method of choosing the pseudo-jet components differs fundamentally from methods that use `KtJet` clustering or the transverse thrust axis of the n jets, in that it is based purely on transverse energy measurements and that no angular information is used whatsoever. This has important consequences for the $\Delta\phi(j_1, j_2)$ of the pseudo-jets, as discussed below.

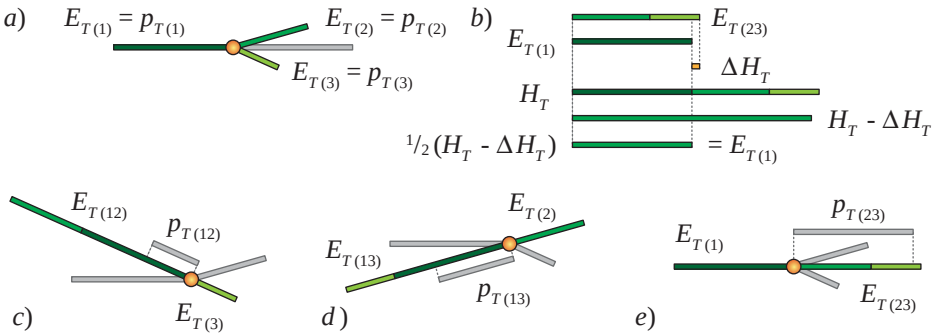

Figure 3: The ΔH_T jet clustering method illustrated. a) A QCD-like three jet event as viewed in the transverse (x-y) plane. Note the original (balancing) jet indicated in grey; b) Calculation of the numerator of α_T using the minimum ΔH_T, obtained from the most dijet-like combination $\{1, 23\}$; c) The $\{3, 12\}$ combination using the merging scheme of Equations 10, 11 and 12; d) The same for $\{2, 12\}$; e) The same for $\{1, 23\}$, the most dijet-like combination.

5 Preliminary studies with CSA07 Monte Carlo datasets

We have used the definition of α_T in Equation 13 in a preliminary analysis of the n hadronic jet channel. The Monte Carlo datasets are the same as those used in [1], and the event preselection is essentially the same with the modifications listed in Section 4.1.

All data samples used in this study use events generated with the simulation package PYTHIA, as only the PYTHIA CSA 07 data samples could provide us with sufficient statistics. We note that PYTHIA is known to systematically underestimate the number of jets in a given final state, and therefore tends to produce biased estimates of the number of expected events for a given jet multiplicity. While this could impact estimates of quantities like the S/B for a given jet multiplicity bin, it is expected that the general kinematic properties for a given event topology (jet multiplicity bin) are simulated reasonably well with PYTHIA. We therefore presume that the results presented here, which are purely based on kinematic information of a given event topology, are reliable. Nevertheless, studies using ALPGEN and Madgraph samples with the required statistics are underway. These will be reported in a future note.

The results for 1 fb^{-1} of simulated data are shown in Table 1. Even without optimisation, it can be seen that the approach looks promising, with $S/B = 7.0$ and $S/\sqrt{B} = 128$ after the $\Delta\phi$ cut. This is comparable to the dijet analysis, but with roughly five times the signal yield. Plots of the pseudo-jet α_T and $\Delta\phi$ for the $n = 4$ system are shown in Figures 4 and 5, respectively. Although we only show results for the $n = 4$ system, the same features are found for each n-jet topology. The strong peak and sharp edge at $\alpha_T = 1/2$ persist, becoming slightly less distinct and favouring lower α_T values as n increases. Likewise, the slope of signal-like events tends to get steeper as n increases.

We also note that, as shown in Figure 5, the ΔH_T transverse energy clustering does not appear to always reconstruct a back-to-back system for QCD events. Considering our previous discussion of the min. ΔH_T clustering method, this is perhaps unsurprising, in that no angular information is used when clustering the jets into pseudo-jets. We can interpret this as saying that phase space and energy mismeasurements are conspiring to produce the incorrect (i.e. non-back-to-back) pseudo-dijet system, or that it is non-trivial to construct the correct pseudo-dijet system from these events that would otherwise pass the acoplanarity cut. Either way, it perhaps does not make sense to consider the acoplanarity cut with the min. ΔH_T clustering method, especially as the α_T cut appears to retain its background rejection power at large jet multiplicities. It would be interesting to compare the $\Delta\phi$ plots for pseudo-dijets constructed with `KtJet` or transverse thrust axis clustering, and also the corresponding signal/background yields produced by these methods as n increases, as these clustering methods place constraints on the event shape. Signal events, for which the event topologies should essentially be random, will not suffer

Table 1: Number of events for $1\,\text{fb}^{-1}$ of simulated data passing successive cuts of $H_T > 500\,\text{GeV}$, $\alpha_T > 0.55$, $0 < \Delta\phi < \frac{2\pi}{3}$ after the n jet preselection described in cuts [1] and Section 4.1 have been applied.

n	Cut	QCD	$Z \to \nu\bar{\nu}$	$t\bar{t}$, W, Z	LM1
2	H_T	3.3×10^6	245	2414	1770
	α_T	0	58.8	20.4	440.0
	$\Delta\phi$	0	57.7	19.2	432.7
3	H_T	6.8×10^6	213	5669	3071
	α_T	24.0	64.4	49.9	852.5
	$\Delta\phi$	24.0	63.9	45.9	837.7
4	H_T	4.0×10^6	86.0	7078	2510
	α_T	2.5	24.5	41.8	676.5
	$\Delta\phi$	2.5	24.0	41.4	668.2
5	H_T	1.0×10^6	19.2	4710	1350
	α_T	21.5	5.8	16.4	295.3
	$\Delta\phi$	21.5	5.8	16.1	290.3
6	H_T	1.8×10^5	2.6	2105	552.5
	α_T	0.4	0.8	8.4	103.1
	$\Delta\phi$	0.4	0.8	8.2	101.0
Total	α_T	48.4	154.3	136.9	2367.4
	$\Delta\phi$	48.4	152.2	130.8	2329.9

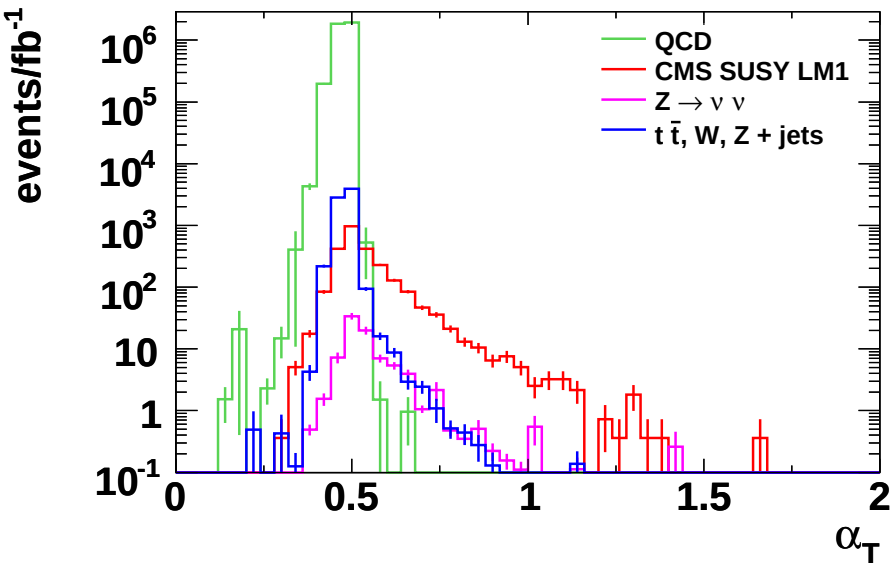

Figure 4: Plot of α_T, as constructed with the min. ΔH_T transverse energy clustering method, for the hadronic $n = 4$ system after the preselection cuts up to and including $H_T > 500\,\text{GeV}$, as outlined in [1] and Section 4.1.

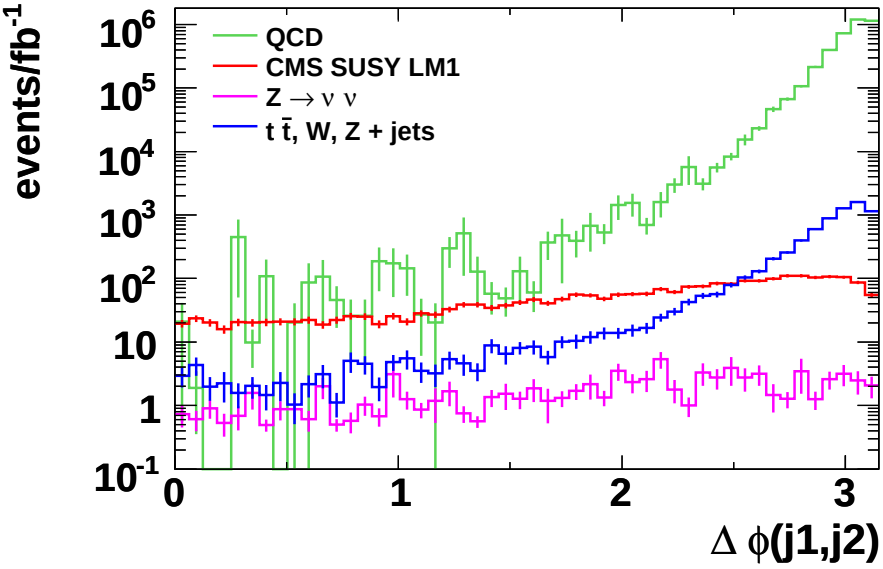

Figure 5: Plot of $\Delta\phi$ of the pseudo-dijets constructed with the min. ΔH_T transverse energy clustering method for the $n = 4$ hadronic jet system after the preselection cuts up to and including $H_T > 500\,\text{GeV}$, as outlined in [1] and Section 4.1.

unduly from the minimised ΔH_T method as the largest numerator of α_T is always selected.

In the context of the dijet system, it is important to again emphasise that the $n = 2$ jet topology appears to be a very special case. While for this jet multiplicity bin the power of α_T mainly stems from angular measurements of the jets (i.e. $\Delta\phi(j_1,\, j_2)$), for $n > 2$ topologies the measurements of the jet energy become the dominant source of systematic uncertainties. Therefore, the very sharp edge of the α_T distributions for $n > 2$ QCD jet multiplities is by no means a trivial observation.

5.1 The self-protection of α_T against jet mismeasurement

We have briefly investigated the robustness of α_T to detector mis-measurements by smearing the energy and momentum of jets in the signal and background Monte Carlo datasets featured in the analysis above, and comparing the performance of an α_T-based analysis and a more traditional, calometric $\not\!\!E_T$/multijet analysis. To do this, we drew inspiration from the $n \geq 3$ jet supersymmetry search presented in [4] (as referenced in [3]), where an explicit cut on $\not\!\!E_T$ ($\not\!\!\mathbf{H}_T$) is applied. For the comparison we present below, we chose the following cuts:

- High-Level Trigger path: `HLT2JET`;
- 10 GeV lepton veto;
- Between 3 and 6 (inclusive) good jets ($E_T^j > 50$GeV and $F_{\text{EM}}^j < 0.9$), with $|\eta^{j_1}| < 2.5$;
- $H_T > 500\,\text{GeV}$, $|\not\!\!\mathbf{H}_T| > 250\,\text{GeV}$;
- $\Delta\phi(\not\!\!\mathbf{H}_T, \mathbf{p}_T^{j_i}) < 0.3$ rad., where $i = 1, 2, 3$;
- $R1 = \sqrt{(\delta\phi_1 - \pi)^2 + \delta\phi_2^2} > 0.5$ rad. and $R2 = \sqrt{(\delta\phi_2 - \pi)^2 + \delta\phi_1^2} > 0.5$ rad.,

where $\delta\phi_i = \Delta\phi(\not\!\!\mathbf{H}_T, \mathbf{p}_T^{j_i})$. The major change from the TDR-style analysis is the use of $\not\!\!\mathbf{H}_T$ instead of the calometric $\not\!\!E_T$. It should be noted that these cuts have not been optimised in terms of the signal yield or the signal-to-background ratio, as we are only interested in the relative performance of the analyses as the jet smearing is increased. The α_T analysis was carried out with the pre-selection cuts of Section 4.1 and the $\alpha_T > 0.55$ cut for events containing 3 and 6 (inclusive).

We applied up to 20% Gaussian smearing, in steps of 2%, to the E and $|\mathbf{p}|$ of all jets identified in the MC dataset ntuples, and calculated the signal-to-background ratio obtained from the analyses for each smearing bin. We then

plotted the S/B of each bin, normalised to the S/B of the 0% bin, for the α_T analysis and the TDR-style analysis. This is shown in Figure 6. We can see from the plot that both approaches have a similar performance up to around

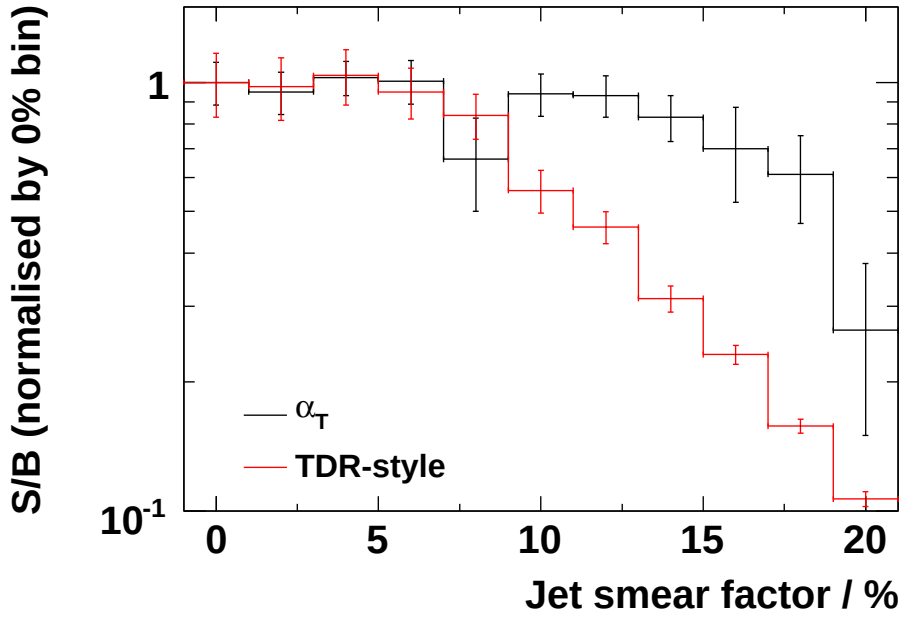

Figure 6: Plot showing an initial indication of the robustness of the α_T approach as compared to a TDR-style approach. The y axis shows the S/B for each level of smearing normalised to that of the 0% bin, to allow a comparison of the performance of the approaches as greater smearing is applied (as opposed to the actual S/B values).

8% smearing [1]. This is perhaps consistent with the fact that we have used $100\,\text{pb}^{-1}$ scenario data samples with the appropriate detector start-up conditions. Beyond 10% smearing, however, the TDR-style analysis performance degrades when compared with that of α_T, up until 20% smearing. While this represents merely a "toe in the water" in terms of robustness studies, as an initial comparison of the approaches it is interesting to see that α_T appears to hold up even with extreme jet mismeasurement. This should certainly be the subject of further investigation.

6 Generalising the α_T approach to kinematics-based searches

As can be seen from Equation 13, α_T is essentially a cut on $|\not{H}_T|/H_T$ kept "safe" by a kinematic constraint on the n jets – in this case ΔH_T, which should be minimised for a balanced (pseudo-)dijet system. This suggests that other combinations of the same kinematic variables may be worthy of investigation. Though ΔH_T and $|\not{H}_T|$ are correlated, we see that the linear combination of H_T and $\Delta H_{T(n)}$ in the numerator will always favour lowering $\alpha_{T(n)}$. This somewhat conservative approach will understandably lower the signal yield while enhancing the self-protection against mismeasured QCD events. One could therefore imagine modified versions of $\alpha_{T(n)}$ which also have self-protecting properties, as long as the numerator in the ratio decreases at least as quickly as the denominator. To demonstrate this principle, we define:

$$\beta_T = \frac{\frac{1}{2}\left(H_T - \Delta H_{T(n)}\right)}{H_T - |\not{H}_T|} \tag{14}$$

and

$$\gamma_T = \frac{\frac{1}{2}\sqrt{H_T^2 - \Delta H_{T(n)}^2}}{\sqrt{H_T^2 - |\not{H}_T|^2}}, \tag{15}$$

[1] We note the dip in the α_T performance in the 8% bin itself, but the overall trend is consistent if one considers the larger error bars on the α_T S/B value for that particular bin.

where we keep the factor of $1/2$ for consistency with α_T. We repeated the analysis described in Section 5 for each new variable, cutting on $\beta_T > 0.8$ and $\gamma_T > 0.6$ respectively, and then on $\Delta\phi$. These unoptimised values were chosen to reflect the kinematic loosening of the new observables. Preliminary results are shown in Table 2, and plots of β_T and γ_T for the $n = 4$ hadronic jet systems are shown in Figures 7 and 8.

Table 2: Number of events for 1 fb^{-1} of simulated data passing successive cuts of $H_T > 500$ GeV, $\beta_T > 0.8$ or $\gamma_T > 0.6$ and $\Delta\phi < \frac{2\pi}{3}$ after the n jet preselection cuts [1] and Section 4.1 have been applied.

		$\beta_T > 0.8$				$\gamma_T > 0.6$			
n	Cut	QCD	$Z \to \nu\bar{\nu}$	$t\bar{t}$, W, Z	LM1	QCD	$Z \to \nu\bar{\nu}$	$t\bar{t}$, W, Z	LM1
2	β_T/γ_T	2.1	101.8	52.1	754.1	1.5	80.8	30.4	600.4
	$\Delta\phi$	2.1	92.4	37.8	672.6	1.5	80.8	30.4	600.4
3	β_T/γ_T	29.0	105.4	122.3	1339.3	6.0	69.8	47.9	916.3
	$\Delta\phi$	27.5	88.4	82.4	1174.9	6.0	69.8	47.7	914.9
4	β_T/γ_T	13.7	44.2	91.4	1068.5	2.5	21.1	26.9	556.4
	$\Delta\phi$	7.7	37.0	76.6	940.5	1.0	21.1	26.9	555.0
5	β_T/γ_T	24.0	7.9	38.0	462.7	21.5	4.0	7.9	176.0
	$\Delta\phi$	22.0	7.5	28.9	408.6	21.0	4.0	7.9	176.0
6	β_T/γ_T	2.5	0.9	16.2	151.5	0.4	0.3	2.8	46.5
	$\Delta\phi$	2.5	0.9	13.6	138.1	0.4	0.3	2.8	46.5
Total	β_T/γ_T	71.3	260.2	320.0	3776.1	31.9	176.0	115.9	2295.6
	$\Delta\phi$	61.8	226.2	239.3	3334.7	29.9	176.0	115.7	2292.8

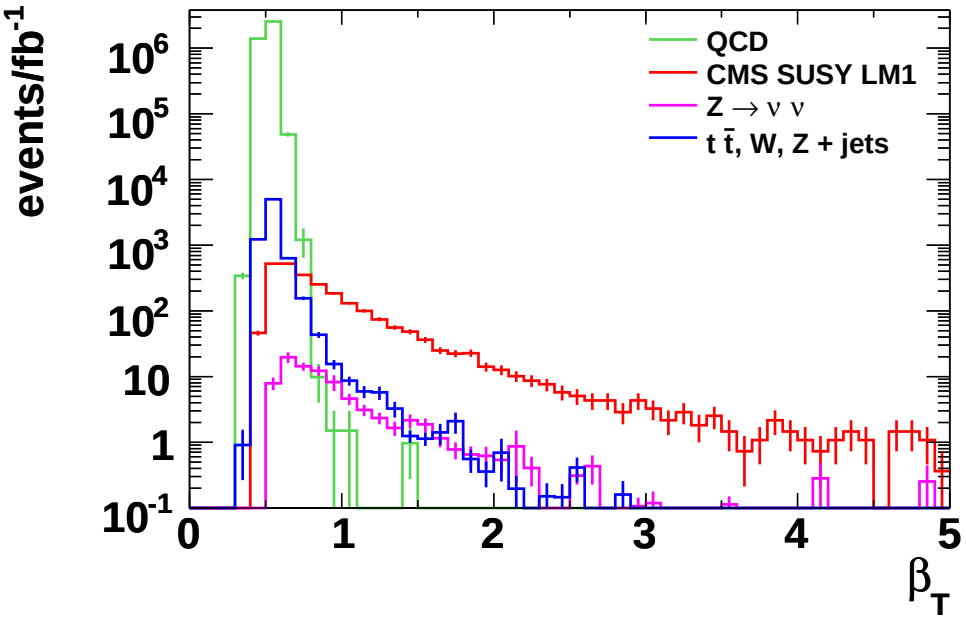

Figure 7: Plot of β_T for the $n = 4$ hadronic jet system after the preselection cuts described in [1] and Section 4.1. Note that the x axis extends to 5.

The β_T approach, after the (largely ineffective) $\Delta\phi$ cut, has $S/B = 6.3$ and $S/\sqrt{B} = 145$ and, as expected, a 50% increase in the signal yield compared to α_T. This is to be compared with $S/B = 7.1$ and $S/\sqrt{B} = 128$ for γ_T, which are very similar to the results for α_T, but using a tighter cut value.

We note that α_T, β_T and γ_T can be parameterised in terms of ratios of $\Delta H_{T(n)}$, $|\not{\mathbf{H}}_T|$ and H_T. For example,

$$\alpha_T = \frac{1}{2} \cdot \frac{H_T - \Delta H_{T(n)}}{\sqrt{H_T^2 - |\not{\mathbf{H}}_T|^2}} = \frac{1}{2} \cdot \frac{1 - \Delta H_{T(n)}/H_T}{\sqrt{1 - |\not{\mathbf{H}}_T|^2/H_T^2}}. \tag{16}$$

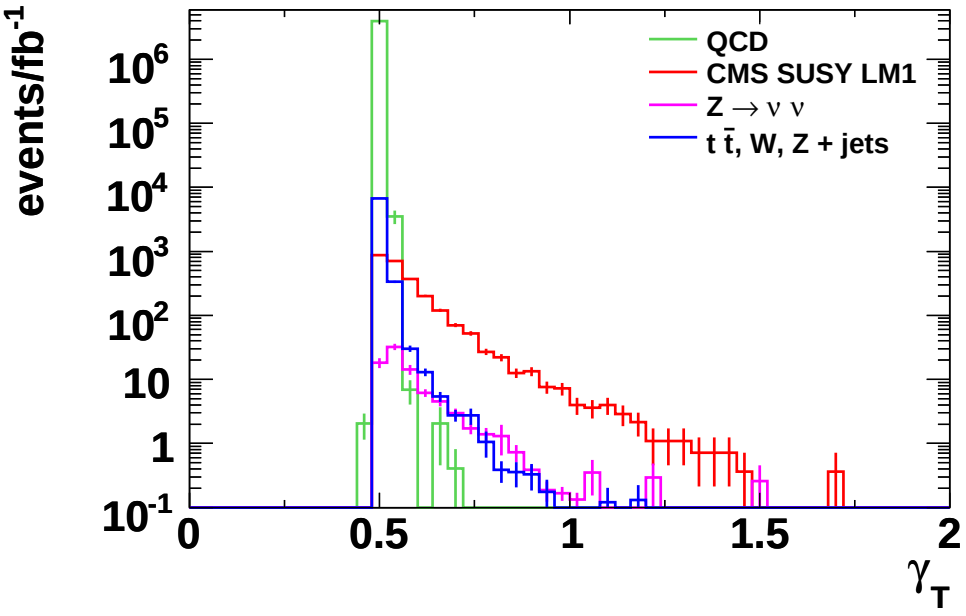

Figure 8: Plot of γ_T for the $n = 4$ hadronic jet system after the preselection cuts described in [1] and Section 4.1.

Thus, without the ΔH_T part, α_T is essentially a cut on the ratio of $|\not{H}_T|$ and H_T. We have therefore plotted $\Delta H_T / H_T$ against $|\not{H}_T|/H_T$ for the $n = 4$ hadronic jet system in Figures 9, 10, 11 and 12, showing where α_T, β_T and γ_T are cutting. Figure 10 is the most interesting, as we note that a cut on $|\not{H}_T|/H_T > 0.5$ would remove most QCD events with the exception of those where ΔH_T and $|\not{H}_T|$ are highly correlated. We can then ask whether there is a more effective way to remove these events without resorting to α_T, which as shown in Figure 9, reduces the signal yield. Initial studies using a modification of the $\Delta\phi(\not{H}_T, \mathbf{p}_T^j)$ cut have shown that indeed there could be. This will be the subject of a future note.

7 Conclusions and Outlook

At first glance, the approach suggested here for generalising the α_T observable used in the hadronic dijet analysis to n-jet event topologies appears to offer a promising, robust way of maintaining the signal-to-background ratio of the approved dijet analysis, while increasing the signal yield by a factor of five.

The strategy also appears to have highlighted the potential of a class of self-protecting observables that mitigate for fake missing transverse energy caused by detector mismeasurements and noise, self-imposed cut choices, or incorrectly defined n-jet systems (i.e. the inclusion of underlying-event jets). However, much work remains to be done:

- The kinematics of the α_T variable, and the nature of the ΔH_T clustering method, needs to be further understood. In particular, the mechanism by which α_T appears to self-correct even when an incorrect pseudo-dijet system is constructed needs to be exploited further, in terms of the relationship between $\Delta H_{T(n)}$ and $|\not{H}_T|$;
- Other α_T-like variables, like those suggested in Section 6, need to be explored in terms of their utility in early SUSY searches.
- Comparisons with TDR-style analyses, and an appreciation of the relationship between ΔH_T and $\not{H}_T$, suggest that there could be other avenues to explore calometric-$\not{E}_T$ independent searches, particularly with reference to the $\Delta\phi(\not{H}_T, \mathbf{p}_T^j)$ cut and simple cuts on $|\not{h}_T|$.
- Methods for constraining the *real* $\not{H}_T$ backgrounds need to be established for the n-jet case. A particularly interesting question is how the ABCD method of [1], which relies on the η of the leading jet, may be extended to the clustered pseudo-dijet system where η cannot be defined. Initial studies have also shown that the $t\bar{t}$ SM background could be particularly problematic for the $n = 3, 4$ case.

These issues should form the basis of future analysis efforts.

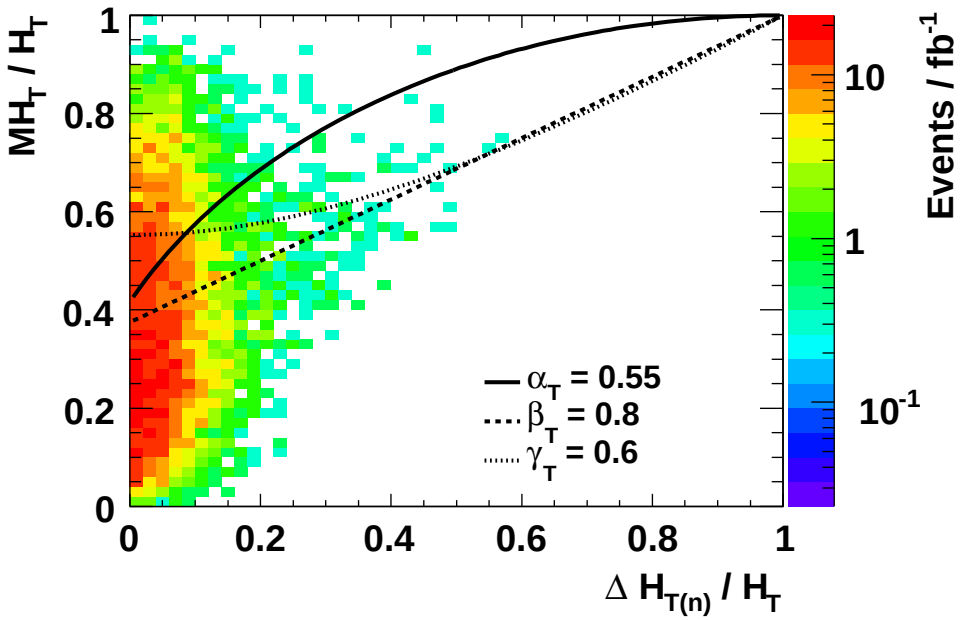

Figure 9: Plot of $\Delta H_{T(n)}/H_T$ against $\not{H}_T/H_T$ for events passing the preselection cuts described in [1] and Section 4.1 in the $n = 4$ hadronic jet system, LM1 dataset.

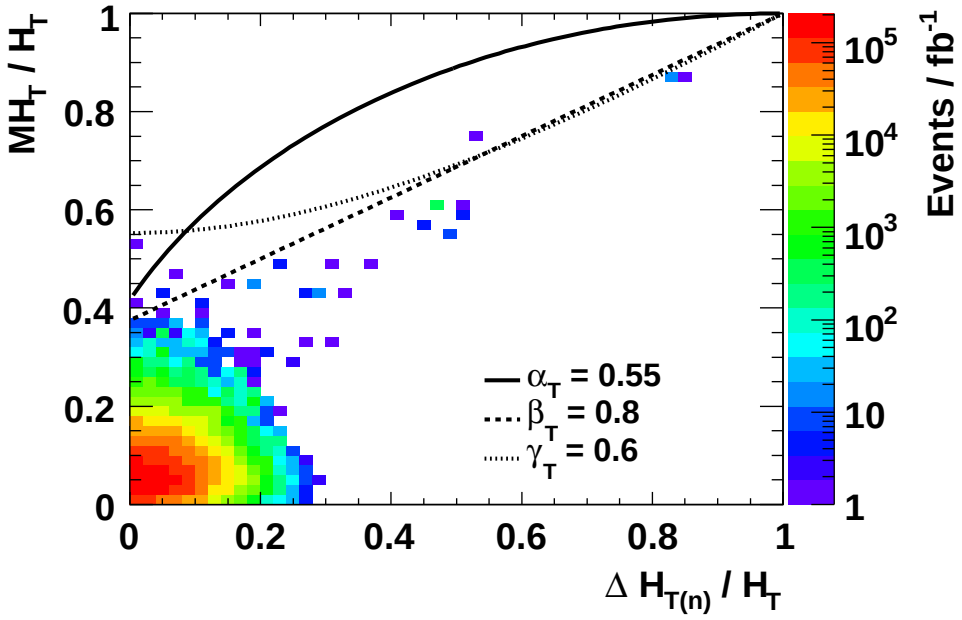

Figure 10: Plot of $\Delta H_{T(n)}/H_T$ against $\not{H}_T/H_T$ for events passing the preselection cuts described in [1] and Section 4.1 in the $n = 4$ hadronic jet system, QCD (Gumbo) dataset. Note that, generally speaking, when $|\not{H}_T|/H_T > 0.5\,|\not{H}_T|$ and $\Delta H_{T(n)}$ appear to be strongly correlated. This is also observed for other n-jet topologies, though is less obvious as n increases.

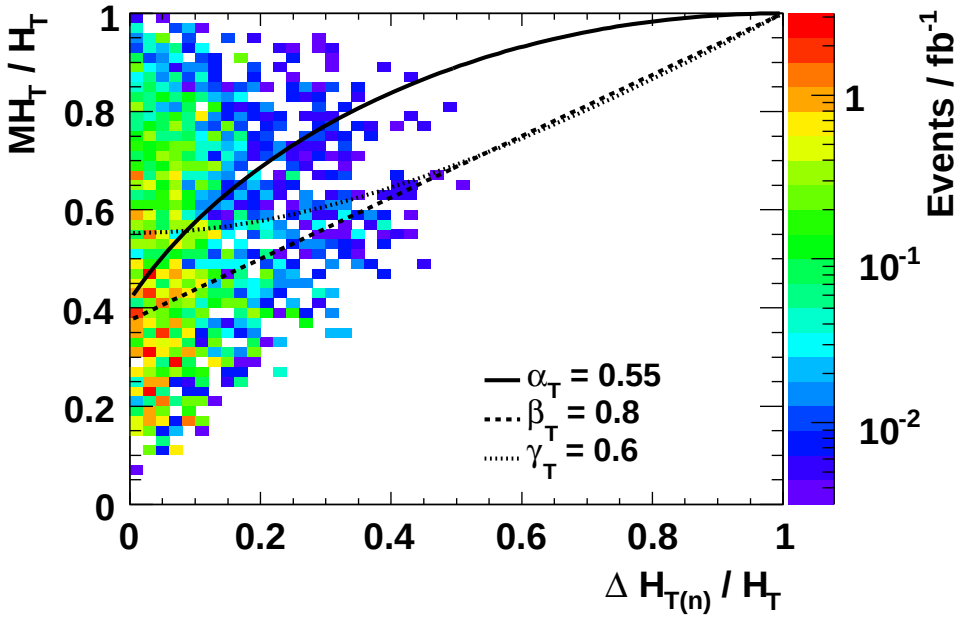

Figure 11: Plot of $\Delta H_{T(n)}/H_T$ against $\not{H}_T/H_T$ for events passing the preselection cuts described in [1] and Section 4.1 in the $n = 4$ hadronic jet system, $Z \to \nu\bar{\nu}$ dataset.

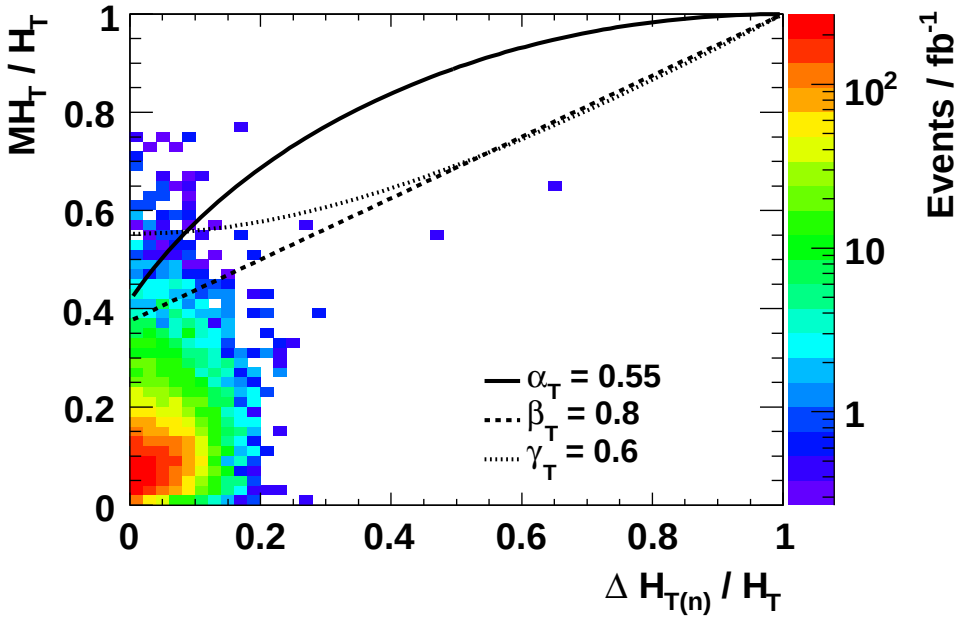

Figure 12: Plot of $\Delta H_{T(n)}/H_T$ against $\not{H}_T/H_T$ for events passing the preselection cuts described in [1] and Section 4.1 in the $n = 4$ hadronic jet system, $t\bar{t}, W, Z +$ jets dataset.

Acknowledgements

The results presented in this note have greatly benefitted from many discussions and interactions with Teruki Kamon and David Stuart on the properties of α_T.

References

[1] H.Flaecher, J.Jones, T. Rommerskirchen, M.Stoye, *"SUSY Search with Dijet Events"*, **CMS AN-2008/071**.

[2] L.Randall, D.Tucker-Smith, *"Dijet Searches for Supersymmetry at the LHC"*, `arXiv:0806.1049`.

[3] The CMS Collaboration, G. L. Bayatian et al: *"CMS Technical Design Report, Vol. II: Physics Performance"*, J. Phys. **G34** (2007) 995-1579.

[4] M. Spiropulu, T. Yetkin, *"Inclusive Missing Transverse Energy + multijet SUSY search at CMS"*, **CMS AN 2006/089**.